Chemical Engineering Journal 150 (2009) 316–322

Contents lists available at ScienceDirect

Chemical Engineering Journal

journal homepage: www.elsevier.com/locate/cej

Study of the bioaccumulation kinetic of lead by living aquatic macrophyte *Salvinia auriculata*

F.R. Espinoza-Quiñones*, A.N. Módenes, L.P. Thomé, S.M. Palácio, D.E.G. Trigueros, A.P. Oliveira, N. Szymanski

Department of Chemical Engineering - Postgraduate Program - NBQ, West Parana State University, Campus of Toledo, rua da faculdade 645, Jd. Santa Maria, 85903-000 Toledo, PR, Brazil

ARTICLE INFO

Article history:
Received 7 November 2008
Received in revised form 19 December 2008
Accepted 5 January 2009

Keywords:
Salvinia auriculata
Lead
Phytoaccumulation
SR-TXRF technique
Non-structural kinetic model

ABSTRACT

In the present work, the lead phytoaccumulation by living free floating aquatic macrophytes *Salvinia auriculata* was investigated in a greenhouse. These plants were grown in lead-doped hydroponic solutions forming, as a function of time, six collections of nutrient media, roots and leaves of plants from a batch system. The synchrotron X-ray radiation fluorescence technique was used in order to determine element concentrations in the nutrient media, dry roots and aerial parts of plant. The aquatic plant-based lead removal data were described by using a non-structural kinetic model. According to the experimental data, both adsorption and bioaccumulation mechanism are present and a competition between the phosphorus macronutrient and lead for plant growth was observed, when great concentration of lead in roots is present. The non-structural kinetic models have shown good agreement with the lead uptake experimental data in all the investigated cases. The results of living macrophytes *S. auriculata*-based-metal bioaccumulation kinetic parameters can be used in artificial wetlands to predict the heavy metal removal dynamics from wastewaters.

© 2009 Elsevier B.V. All rights reserved.

1. Introduction

The environmental impact and building up of heavy metals in flora and fauna in aquatic ecosystem has been a cause of great concern in recent years. Heavy metals are introduced into environment as a result of industrial activities and technological development, which have caused a decrease in the quality of water, bringing up harmful effects to the flora and fauna and consequently damaging the human health, by it's accumulation in the food chain and persistence in nature [1,2]. Lead pollution results from the textile dyeing, ceramic and glass industries, petroleum refining, battery manufacture and mining operations [3].

Nowadays, many conventional methods, that involve physical, chemical, and biochemical processes such as ion exchange, reverse osmosis, electrolysis, precipitation and adsorption, are available in order to remove toxic metals from polluted water [4–7].

Biological methods, called biosorption, have been recommended as cheaper and more effective techniques for the heavy metal ion removal and recovery from aqueous solutions [8,9]. Based on this technique, non-living plants can be used for heavy metal removal due to their low costs, free availability and easy regeneration. Among these new techniques, the phytoremediation has become an alternative method to remove heavy metal and other pollutants from waste waters [7]. Aquatic macrophytes are known to remove metals by surface adsorption and/or absorption and incorporate them into their own system or store them in a bound form [10]. The type of aquatic plant used in the treatment procedure can make a significant difference in pollutant removal [11,12]. Furthermore, the knowledge of metal kinetic bioaccumulation parameters for aquatic plants has become crucial for plant-based treatment design to improve the metal removal efficiency in artificial wetlands [13].

The main purpose of this work was to evaluate the lead ion removal by the floating aquatic macrophytes *Salvinia auriculata*. Several different bioaccumulation models were tested within a system of algebric/differential equations, containing also the global biomass balance and lead accumulated concentration in the biomass. The identification of the lead bioaccumulation parameters was based on the particle swarm optimization procedure.

2. Materials and methods

2.1. Chemicals

All the chemicals used were of analytical-reagent grade. Some macro- and micro-nutrients were prepared, according to the Clark's

* Corresponding author. Tel.: +55 45 3379 7092; fax: +55 45 3379 7002.
E-mail addresses: f.espinoza@terra.com.br, espinoza@unioeste.br (F.R. Espinoza-Quiñones).

1385-8947/$ – see front matter © 2009 Elsevier B.V. All rights reserved.
doi:10.1016/j.cej.2009.01.004

hydroponic solution [14]. For the growing media, six 1 L single macronutrient solutions of $Ca(NO_3)_2{\cdot}4H_2O$ (1 M), KNO_3 (1 M), KCl (1 M), NH_4NO_3 (1 M), $MgSO_4{\cdot}7H_2O$ (1 M), and $Ca(H_2PO_4)_2{\cdot}H_2O$ (0.023 M) were separately prepared using deionized water, while a 1-L multi-chemical micronutrient solution containing H_3BO_3, $ZnSO_4{\cdot}7H_2O$, $(NH_4)_6Mo_7O_{24}{\cdot}4H_2O$, $CuSO_4{\cdot}5H_2O$, $MnCl_2{\cdot}4H_2O$, and $FeCl_3{\cdot}6H_2O$ with different concentrations (19, 2, 0.086, 0.5, 7, and 40 mM for each chemical, respectively) were also prepared in a similar way. Diluted stock solutions (1:1000, v/v) were used to prepare a hydroponics media [14], containing macro- and micro-nutrients for aquatic macrophytes cultivation.

Stock solution of 1.0 g Pb^{2+} L^{-1} was also prepared from $Pb(NO_3)_2$, diluted in deionized water and stored in a 2-L volumetric flask. Moreover, multi-elemental stock solutions have been also prepared from mono-elementary standard solutions of some light and heavy elements, mixed in different concentrations, in order to cover an energy wide region of K and L X-ray series, respectively, and to obtain the sensitivity curves from the synchrotron radiation reflection X-ray fluorescence technique (SR-TXRF) [15,16].

2.2. Sampling and preliminary tests

Aquatic macrophytes *S. auriculata* plants were collected from a natural shallow pond near Palotina city, which is located in the west region of the Brazilian Paraná state, and put into clean 300 L boxes containing tap water from a greenhouse for experimental purposes. After collection, aquatic macrophytes *S. auriculata* were thoroughly cleaned in running tap water, in order to eliminate any remains of sediment and particles. Only healthy plants with uniform size and weight were chosen for the experimental tests and metal uptake experiments.

Growth and toxicological tests were performed in 2 L acid-washing polyethylene containers at the same experimental conditions such as room temperature, solar luminosity, nutrient solution and time. A set of hydroponic solutions supplied with lead concentrations in the range from 1.0 to 10 mg L^{-1} was prepared in order to perform the toxicological test, using around 50 g plants. In a similar procedure, growth test was carried out using only hydroponic solution without any lead ions in it and 50 g healthy plants.

2.3. Lead uptake experiment

Clean and healthy young macrophytes *S. auriculata* were used in lead uptake experiment, which was conducted using 8 L acid-washed plastic containers. As metal-doped nutrient medium, 5 L hydroponic solutions supplied with a lead concentration of 2.0 mg Pb^{2+} L^{-1} was put in each container, where approximately 30 g plants were grown during 29 days in a greenhouse. During the experiment, the solution temperature and pH were measured daily, while the solution volume was monitored and deionized water was added to compensate for the loss by evaporation.

Seven collection times of 1, 2, 5, 8, 15, 22 and 29 days were set up. During each collection time, a triplet of containers was taken out from the greenhouse and, afterwards an entire plant with 100 mL of nutrient solution from each recipient was collected and stored for subsequent metal analysis. Plants were rinsed in deionized water and then allowed to dry at room temperature for a few minutes, and then were weighed and stored. Previous to the drying process of the biomass, the plant was cut and divided into roots and leaves, and weighed. Each part of the plant was oven-dried at 80 °C for 72 h, weighed and ground. A digestion procedure was carried out by the addition of 5.0 mL (65%) HNO_3 and 0.5 mL (30%) H_2O_2 to 0.5 g of dry leaves and roots and by heating it on a hot plate [17,18]. Finally, deionized water was added to the digested sample, in order to reach a total volume of 10 mL and then it was stored [19].

2.4. SR-TXRF measurements

For element analysis, an internal certificated standard (10.0 mg Ga L^{-1}) was added to each 2 mL sample (water or plant) and stored in a glassware. Using a digital micropipette, an aliquot of 5 μL was deposited on a pre-cleaned acrylic disk (ϕ 30 mm, 3.0 mm thick) and dried at room temperature inside a clean box, obtaining a thin spot of dry residue for SR-TXRF analysis. Blank control samples (deionized water and all reagents) and mixed multi-element standard samples [19] were prepared by the same procedure.

In order to measure the biomass-accumulated metal concentration and metal concentration in nutrient solution, the SR-TXRF technique was used. The SR-TXRF measurements were carried out using a polychromatic X-ray beam, with beam energy from 2 up to 20 keV, from the D09-XRF beam-line, of the Brazilian Light Synchrotron Laboratory (LNLS) [20]. Each reflector disk containing the evaporation-residual sample was put in an X-ray total reflection position and the acquisition time was set at 100 s, except for standard samples where it was set at 300 s. A HP-Ge detector, with 160 eV FWHM at Mn Kα line, was used for X-ray detection. SR-TXRF element sensitive curve for the K and L X-ray series was obtained using five well-known concentration levels of mixed multi-element standards.

2.5. Parameter identification method

The identification of metal bioaccumulation kinetic parameter values can be considered as a key step in the model development procedure. In this work, the estimation of model parameters was performed by using the particle swarm optimization (PSO) global method, created by Kennedy and Eberhart [21]. The PSO method is similar to the evolutionary algorithms (EA) and is based on a population of individuals, called particle swarm. However, the only difference between EA and PSO is in the space localization of individuals (particles) recognized by the operator speed. In genetic algorithms GA, the individuals pass through the operator reproduction, mutation and election [22].

In PSO method, a vector is attributed to each individual of the population (particle) that corresponds to a possible solution of the problem. Each particle possesses a position and a speed in the search space, with dimensions equal to the number of parameters of the problem, resulting in a swarm with its size equal to the number of particles. The particles act under three influences represented by vectors which determine its speed and position in the space: (i) vector of current position; (ii) vector of better position for the particle; (iii) vector of better position for the swarm. The current position of the particle, given by Eq. (1), with predetermined search range is used for initialization of the population:

$$\vec{X}_i^{(k)} = \vec{X}_{\min} + \lambda(\vec{X}_{\max} - \vec{X}_{\min}) \quad (1)$$

The speed and the position of particles at each iteration are updated as follows:

$$\vec{V}_i^{(k+1)} = \omega^{(k)}\vec{V}_i^{(k)} + c_1\lambda_1(\vec{X}_{i\text{best}}^{(k)} - \vec{X}_i^{(k)}) + c_2\lambda_2(\vec{X}_{g\text{best}}^{(k)} - \vec{X}_i^{(k)}) \quad (2)$$

The first-term of Eq. (2) keeps each particle in the previous direction; the magnitude of this vector depends on the inertia factor (ω), the variable that controls the degree of convergence of the search. The second- and third-terms represent the influence of the best individual position and the best position of the swarm, respectively, and their magnitudes depend on the values of acceleration constants (c_1 and c_2) and variables (λ_1 and λ_2). These variables are normalized in the interval of 0–1. The values of constants used in the identification procedure were as follows $c_1 = 1$ and $c_1 = 2$. In this work an appropriate value for the inertia factor was obtained by

applying the following equation:

$$\omega^{(k)} = \omega_{\text{initial}} + (\omega_{\text{end}} - \omega_{\text{initial}}) \left(\frac{k-1}{K-1} \right) \quad (3)$$

where $\omega_{\text{initial}} = 0.9$ and $\omega_{\text{end}} = 0.4$.

From then on, the particles "are flying" to new positions according to the following equation:

$$\vec{X}_i^{(k+1)} = \vec{X}_i^{(k)} + \vec{V}_i^{(k+1)} \quad (4)$$

For the initialization of the population, the following parameter values are predefined: particle number, number of iterations, number of parameters, inertia factors, acceleration constants and the search limit. The fitness of each particle is measured in accordance with statistical criterion (the last square method as objective function). During the search of the objective function minimum by PSO algorithm, 300 particles and 25 iterations were used. An AMD Sempron computer, with 2.8 GHz and 512 Mb of RAM memory was used.

When the specified number of iterations is reached, the best search solution is used as information in the process of restriction of the search space, where the most sensible parameters are considered. This evaluation of the parameter sensitivity is possible in a graphical dialog, by using Maple® software. Moreover, the search for the best parameter values was guided by the microbiological meaning of each parameter and served as a base for predetermining the parameter search range, where the best evaluated values were preserved, after repeated searches and analyses of the obtained results. The end of the search is determined by the better global position of the swarm. The search stop criterion is given by following conditions:

$$\vec{X}_{i\text{best}}^{(k+1)} = \vec{X}_i^{(k+1)} \text{ if } f(\vec{X}_i^{(k+1)}) < f(\vec{X}_{\text{ibest}}^{(k)}) \quad (5)$$

$$\vec{X}_{g\text{best}}^{(k+1)} = \vec{X}_{i\text{best}}^{(k+1)} \text{ if } f(\vec{X}_{i\text{best}}^{(k+1)}) < f(\vec{X}_{g\text{best}}^{(k)}) \quad (6)$$

3. Results

3.1. Preliminary tests and uptake experiment

The aquatic plant grown in 2.0 mg $Pb^{2+}\,L^{-1}$ concentration has shown similar growth rates compared with those grown in nutrient media without metal. This experimental condition has shown that the lead concentration bellow 2.0 mg Pb L^{-1} did not have toxic effect on plant growth. The growth rate value for *S. auriculata* was about 1.0 g d^{-1} at approximately 20 °C.

The daily solution temperature was varying between 18 and 26 °C, resulting in a mean temperature of 20 °C, during all lead uptake experiment. At the interval of pH values ranging from 3.5 to 5.0, which was observed during all the experiments where the lead precipitation was not expected to occur.

3.2. Element concentrations

The analysis of all SR-TXRF spectra obtained from lead-doped nutritive solution, digested-dry roots and leaves samples were made using the AXIL software [23]. The following elements S, P, K, Ca, Ti, Cr, Mn, Fe, Cu, Zn, Br and Mo, which are present in nutrient solution, and Ga, as internal standard, as well as Pb, as tested metal, were mainly identified by their strong X-ray Kα and Lα lines, as can be seen in Fig. 1. The X-ray energy region of light elements such as C, N, and O, among others, was a non accessible region by the configuration of SR-TXRF spectrometer. In addition, some elements were not possible to identify because of their low concentrations in nutrient solution or dry biomass and the strong X-ray peak interference caused by the main elements in it. Based on the strong X-ray

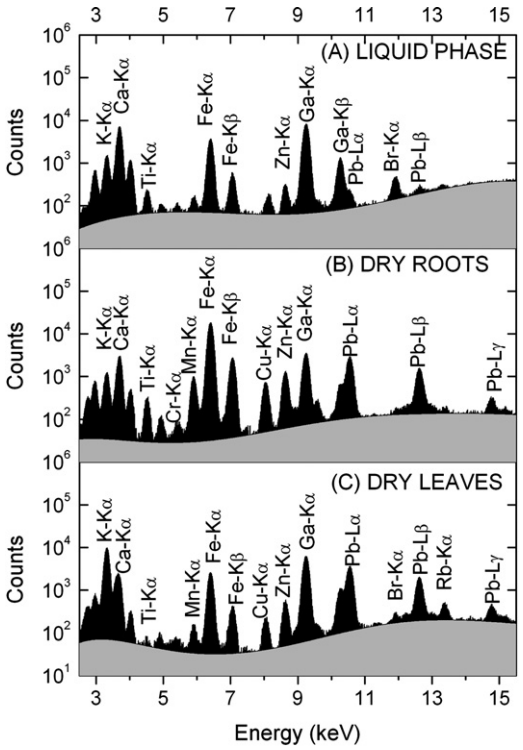

Fig. 1. Three typical SR-TXRF spectra obtained from liquid phase (lead-doped hydroponic solution) and both digestion solutions of dry roots and leaves after 2 d of lead uptake experiment.

Kα peak intensity of known element concentrations in multi element standard samples, the relative-to-gallium sensitivity values were determined for both X-ray K and L series of the SR-TXRF spectrometer and were fitted with an exponential-type functions, as can be seen in Fig. 2, with their adjustable parameters reported in Eqs. (7) and (8). A set of good correlation coefficients and χ^2 values for both sensitivity curves were obtained:

$$S_K(Z) = \exp[-25.6140 + 1.6665Z - 0.0271Z^2] \quad (7)$$

$$S_L(Z) = \exp[-29.9359 + 0.7792Z - 0.0052Z^2] \quad (8)$$

where S_K and S_L represent the relative-to-gallium fluorescent sensitivity for light and heavy elements, respectively, Z is the atomic number.

The element concentration in aqueous solutions (nutritive solution or digested dry roots or leaves) were calculated by using Eq. (9) [18,19,24]. Moreover, the amount of element mass per dry-

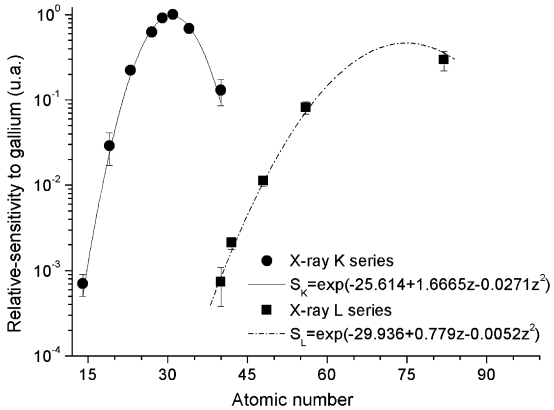

Fig. 2. Relative-to-gallium sensitivity curves for X-ray K and L series of the SR-TXRF spectrometer.

Table 1
Mean concentrations of elements in hydroponic medium. The standard deviations are less than 15%.

Time (d)	Element concentration (mg L^{-1})									
	S	K	Ca	Ti	Cr	Mn	Fe	Cu	Zn	Br
0	3.1	59	144	0.19	0.25	0.23	3.31	0.05	0.3	0.4
1	0.2	58	135	0.54	0.39	0.26	4.33	0.07	0.3	0.4
2	2.9	63	122	0.04	0.25	0.28	1.62	0.05	0.3	0.2
5	1.3	81	207	0.19	0.21	0.28	1.95	0.03	0.2	0.2
8	12.5	65	182	0.21	0.27	0.24	2.36	0.04	0.4	0.2
15	0.1	57	159	0.95	0.20	0.22	4.79	0.03	0.2	0.5
22	0.1	57	156	0.14	0.15	0.16	1.69	0.03	0.2	0.3
29	3.2	52	150	0.85	0.31	0.30	4.66	0.06	0.3	0.5

biomass (roots or leaves) was determined according to Eq. (10), taking account the small dry digested biomass and the final volume of dilution. The results of the mean element concentration are summarized in Tables 1–3. In Table 1, the main macro/micro-element concentrations in the hydroponic medium at each time collection are reported:

$$C_{LP}(z) = \frac{I_Z}{I_{Ga}} \times \frac{C_{Ga}}{S(z)} \quad (9)$$

$$C_{SP}(z) = C_{LP}(z) \times \frac{V}{M} \quad (10)$$

where I represents the fluorescent intensity of the element, C_{LP} is the element concentration for liquid phase, C_{Ga} is the Ga concentration (internal standard), C_{SP} is the element concentration for dry solid phase, M is the initial mass and V is the final volume, before and after acid digestion process, respectively.

3.3. Lead uptake modeling

The modeling of lead removal and lead bioaccumulation data, as shown in Table 4, was based on the lead mass balance and the relation between the increase of biomass as a function of time and the metal concentration reduction from the hydroponic media. The lead bioaccumulation from a nutrient media by living aquatic macrophytes *S. auriculata* has been described by four non-structural kinetic models, Eqs. (11)–(14), but instead of the adsorption rate determination, the accumulated-metal maximum capacity and rate constants of bioaccumulation were estimated. These models resemble the Langmuir-type irreversible, reversible and pseudo-first- and second-interaction models, respectively.

Indeed, there are several mass transfer mechanisms involved in the heavy metal removal process by living microorganism, which cause great difficulties for the modeling of the whole process. Because of this, in other similar works [25,26] a mechanistically classical models of enzymatic and adsorption kinetics have been used, in order to represent the heavy metal bioaccumulation kinetic for living organisms. This way, we have followed the non-living biosorbent action-based adsorption kinetic classical modeling:

$$r(t) = k_1[q_{max} - q(t)]C(t) \quad (11)$$

$$r(t) = k_2[q_{max} - q(t)]C(t) - k_b\,C(t) \quad (12)$$

$$r(t) = k_3[q_{max} - q(t)] \quad (13)$$

$$r(t) = k_4[q_{max} - q(t)]^2 \quad (14)$$

where C (in mg Pb L^{-1}) is the time dependent lead concentration in the liquid phase, r (in mg Pb g^{-1} d^{-1}) is the lead bioaccumulation action rate by the aquatic plant, q (in mg Pb g^{-1}) is the macrophyte-accumulated lead concentration, q_{max} (in mg g^{-1}) is the macrophyte-accumulated maximum lead content constant, k_1 (in L mg^{-1} d^{-1}), k_2 (in L mg^{-1} d^{-1}), k_3 (in d^{-1}), and k_4 (in g mg^{-1} d^{-1}) are the bioaccumulation rate constants, k_b (in L d^{-1} g^{-1}) is the lead desorption rate constant only for mechanistically based reversible kinetic model.

A set of algebraic and ordinary differential equations, given by the Eqs. (15)–(17), that represent the global mass balance and the accumulated metal balance in the biomass was considered to include the time growth of biomass in 30 days of lead uptake experiment. Several polynomial-type functions and segmented curves in different growing phases were tested. Among the all considered functions, the best agreement with the kinetic data was obtained using a third-order polynomial function for the growth data, as shown in Fig. 3. In the non-linear parametrical identification procedure, the maximum lead accumulation and rate constants were

Table 2
Mean element concentrations (μg g^{-1}) in digested dry roots of *S. auriculata* obtained from lead uptake experiment using a hydroponic medium. The standard deviations are less than 15%.

Time (d)	Element concentration (μg g^{-1}) in dry roots of *S. auriculata*											
	P	S	K	Ca	Ti	Cr	Mn	Fe	Cu	Zn	Br	Mo
0	60	664	1117	1643	5.6	1.4	14	261	8	50	1.7	2
1	320	955	3756	5124	11.8	6.8	43	1541	49	74	19.2	95
2	288	509	3371	4545	5.9	5.4	86	1591	64	114	6.1	76
5	415	729	3926	5134	55.9	16.7	22	2412	52	49	22.2	81
8	357	287	2500	3176	8.9	4.2	14	2159	48	33	6.2	143
15	254	260	2499	3198	43.9	4.4	127	1746	44	74	4.1	46
22	221	627	3009	4998	25.1	6.0	156	1834	43	70	5.7	30
29	119	521	3019	2978	10.2	4.7	13	1553	31	25	3.7	21

Table 3
Mean element concentrations (μg g^{-1}) in digested dry leaves of *S. auriculata* obtained from lead uptake experiment using a hydroponic medium. The standard deviations are less than 15%.

Time (d)	Element concentration (μg g^{-1}) in dry leaves of *S. auriculata*										
	P	S	K	Ca	Ti	Cr	Mn	Fe	Cu	Zn	Br
0	1064	295	5,282	1466	7.0	1.8	5.6	150	2.6	37.4	12.5
1	1003	920	8,232	1483	5.1	2.1	8.6	176	3.7	17.1	10.3
2	517	664	5,233	742	1.4	1.4	9.2	64	2.0	11.7	5.1
5	295	1210	7,692	1201	1.7	1.7	4.5	122	5.5	17.8	5.0
8	175	2440	11,956	1576	4.2	3.2	5.8	134	6.3	16.2	6.3
15	233	2247	10,861	1046	0.0	4.0	9.0	146	6.2	16.1	5.6
22	269	2530	11,566	1568	3.0	3.0	19.4	162	5.7	17.6	5.2
29	394	2719	9,302	1205	4.5	3.1	5.6	181	6.5	17.6	6.3

Table 4
Mean mass (±S.D.) of living *S. auriculata* after each collection time and the mean lead (±S.D.) and phosphorus (±S.D.) concentration values determined by SR-TXRF technique. S.D. calculated from three replicates for all cases.

Time (d)	pH	Wet biomass (g)	Lead concentration			Phosphorus concentration	
			Liquid phase (mg L^{-1})	Dry roots (μg g^{-1})	Dry leaves (μg g^{-1})	Dry roots (μg g^{-1})	Dry leaves (μg g^{-1})
0	3.5 ± 0.2	31.9 ± 1.0	1.24 ± 0.06	2.2[a] ± 0.2	1.1[b] ± 0.1	60[a] ± 8	1064[b] ± 103
1	4.2 ± 0.3	31.9 ± 1.0	0.59 ± 0.11	777 ± 46	1.4 ± 0.1	320 ± 30	1003 ± 78
2	4.0 ± 0.2	32.0 ± 1.2	0.47 ± 0.05	737 ± 55	1.3 ± 0.3	288 ± 27	517 ± 79
5	4.3 ± 0.2	33.5 ± 1.5	0.34 ± 0.04	561 ± 64	126 ± 9	415 ± 56	295 ± 36
8	4.6 ± 0.2	35.6 ± 2.1	0.20 ± 0.08	499 ± 28	213 ± 11	357 ± 30	175 ± 23
15	4.8 ± 0.2	39.3 ± 3.7	0.15 ± 0.07	528 ± 32	217 ± 19	254 ± 22	233 ± 31
22	4.9 ± 0.2	41.5 ± 2.2	0.13 ± 0.04	598 ± 33	178 ± 21	221 ± 35	269 ± 23
29	5.0 ± 0.2	42.8 ± 1.3	0.11 ± 0.06	494 ± 28	197 ± 30	119 ± 18	394 ± 51

[a] Concentration found in dry roots of non-treated aquatic plant.
[b] Concentration found in dry leaves of non-treated aquatic plant.

determined and optimized by the particle swarm optimization (PSO) global optimizer, coded in Maple® software, following the description in Section 2.5. The set of equations (Eqs. (11)–(17)) was solved by using Lsode package with Adamsfull method inside the Maple® software:

$$V[C_0 - C(T)] = m(T)q(t) \quad (15)$$

$$\frac{d}{dt}[m(t)q(t)] = m(t)r(t) \quad (16)$$

$$m(t) = 31.53 + 0.392t + 0.015t^2 - 0.00052t^3 \quad (17)$$

where C_0 (in mg L^{-1}) is the initial lead concentration in the liquid phase, m (in g) is the time dependent wet biomass, and V is the total volume (5 L) of the nutrient media.

The living aquatic macrophyte-based lead removal data and their lead bioaccumulation kinetic model results are shown in Fig. 4. The lead bioaccumulation parameters estimated values for each model, obtained during the PSO search by minimizing the objective function, are summarized in Table 5.

4. Discussion

Based on the SR-TXRF results, many micro- and macro-nutrients have been identified and quantified in the liquid and solid phase of samples, as can be seen in Fig. 1 and are reported in Tables 1–4. Some elements introduced in the hydroponic solution, such as Mo and P, which are expected to be present in the spectra, were not possible to quantify because of their very low sensitivity values in the SR-TXRF spectrometer and the overlapping of other strong X-ray lines. However, due to the drying of biomasses and the bioaccumulation processes of the P and Mo elements of at low concentrations in the nutritive medium were enhanced in dry biomass and reported in Tables 2–4.

The analysis of lead uptake experiment by the SR-TXRF technique has allowed the monitoring of time-dependent changes in the amounts of phosphorus and lead concentration taken up by the living roots and stored in leaves. From Table 4, the initial natural amount of lead in dry leaves and roots is negligible. After the first 24 h of lead uptake experiment, an increase of lead concentration in dry roots of 800 μg g^{-1} has been observed, which corresponds to about 50% depletion of lead concentration in nutritive medium. This result indicates that there is a fast mechanism of adsorption between liquid phase and roots, while the bioaccumulation process of lead is apparently much slower. Moreover, during the 5 initial days, the lead concentrations in dry roots have quickly decreased from around 800 to 550 μg g^{-1} and this loss was observed to appear in leaves with an increase of 200 μg g^{-1} after 8 days, within a standard deviation, as can be observed in Fig. 5. This behavior of lead concentration in roots and leaves during the first day of experiment could be explained by the presence of both biosorption and bioaccumulation processes. In contrast to lead concentration behavior, the phosphorus concentrations in leaves have suffered a strong reduction from about 1100 to 200 μg g^{-1} after 5–8 days of experiment, when the phosphorus concentration in dry roots has become

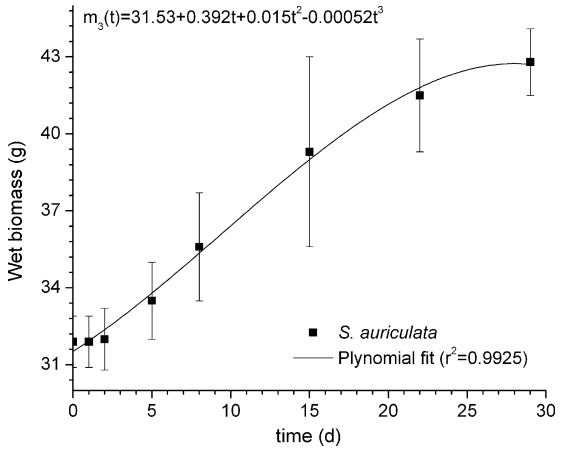

Fig. 3. The behavior of wet biomass and solution temperature as function of time.

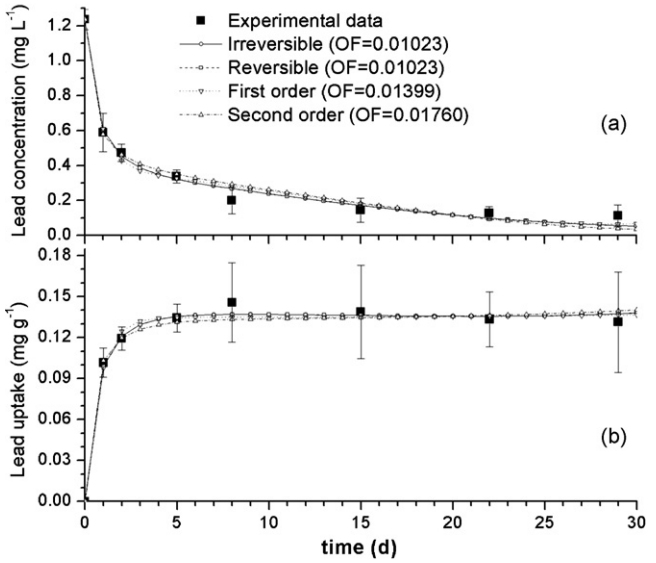

Fig. 4. Experimental data of lead and the fits by non-structural kinetic models. The measured time dependant concentration values of Pb^{2+} in: (a) bulk fluid phase and (b) solid bulk phase are shown as solid-squares. The modeling results as solid, dot, dashed, and dash-dotted lines correspond to the non-structural irreversible, reversible, pseudo-first- and second-interaction models, respectively.

Table 5
Lead bioaccumulation modeling parameters used to represent the lead uptake by *S. auriculata*.

Kinetic model	Maximum lead content (mg Pb g^{-1})	Rate constant	Desorption rate constant (L g^{-1} d^{-1})	Objective function
Reversible	0.1340	2.5560[a]	0.0511	0.01023
Irreversible	0.1140	2.5561[a]		0.01023
Pseudo-first-order	0.120	1.8102[b]		0.01399
Pseudo-second-order	0.1270	10.0[c]		0.01760

[a] k_1 and k_2 in L d^{-1} mg^{-1} Pb.
[b] k_3 in d^{-1}.
[c] k_4 in g d^{-1} mg^{-1} Pb.

maximum, reaching around 350 μg g^{-1}. This feature of phosphorus stored suggests that there is a mobilization of stored phosphorus in leaves and its retranslocation from leaves to roots. After 15 days of experiment, the phosphorus concentrations have gradually increased in leaves, while they have been reduced in dry roots, as can be observed in Fig. 5.

The concentration reduction of phosphorus and increase of lead in a simultaneous way is an indication that there is a competition between the basic phosphorus macronutrient and lead in plant growth, when great concentrations of lead in roots are present. After the consumption of lead concentration from the hydroponic medium, the plant tends to put back the phosphorus concentration by a biosorption process and then the bioaccumulation by the other parts of the plant.

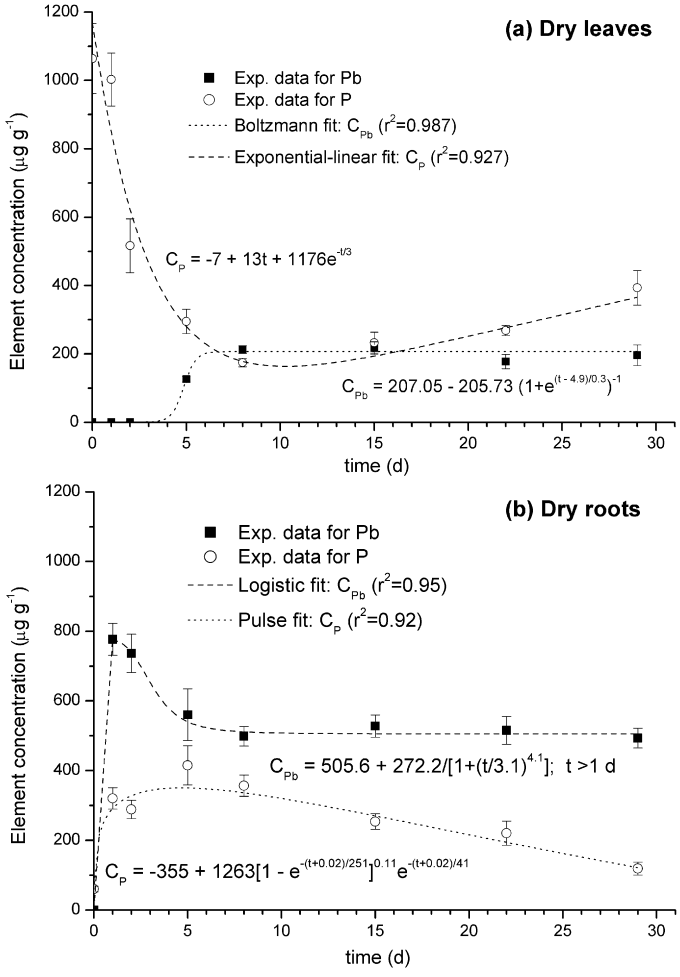

Fig. 5. Behavior of lead and phosphorus concentrations in: (a) dry leaves and (b) dry root biomass as a function of time.

For the determination of the living macrophyte-based-lead bioaccumulation kinetic parameters, it is important to take into account most of the plant's growth parameters, because most of the experimental conditions *in situ* were not controllable, such as the temperature and solar irradiance among other factors. Thus, the growth of living biomass as a function of time was introduced as an important dynamic parameter within a set of equations for the modeling of lead uptake.

According to the PSO method, the lowest objective function (OF) was for both irreversible and reversible models, indicating that the best fit was obtained for both models, as can be seen in Fig. 4. From all the considered models, the optimized maximum lead experimental content onto the plant was about 0.12 mg Pb g^{-1} of wet biomass (see Table 5). While, the optimized rate constant values (k) were about 2.55 L d^{-1} mg^{-1} for both irreversible and reversible biosorption kinetic models, indicating that the lead desorption rate constant value (0.0511 L g^{-1} d^{-1}) can be considered as negligible (the second-term of Eq. (12)) as compared with the lead adsorption one (the first-term of Eq. (12)). Thus, there is no reversible process occurring at the lead uptake by the living aquatic macrophytes *P. stratiotes*. The modeling information about the bioaccumulation dynamics process can be successfully used to plan an industrial effluent treatment, considering the *S. auriculata* as a viable alternative living biosorbent.

5. Conclusion

Below the 2.0 mg Pb^{2+} L^{-1} concentration, there was no impact on aquatic macrophytes growth. According to the experimental data, both adsorption and bioaccumulation mechanism are present. In the first 24 h, a significant lead concentration reduction from the lead-doped hydroponic medium was verified, indicating that the main process was the biosorption one. After first day of experiment, the lead bioaccumulation was also observed and checked by the lead concentration in the leaves.

From the concentration reduction of phosphorus and a simultaneous increase of lead, on the other hand, a competition between the phosphorus macronutrient and lead for plant growth was observed, when great concentrations of lead in roots are present.

Assuming that the lead removal rate is proportional to both bioaccumulation capacity on the macrophytes and the lead concentration in liquid phase, the non-structural kinetics models have shown good results when fitting the lead uptake experimental data in all the investigated cases.

The aquatic macrophyte *S. auriculata* has shown a good metal removal capacity during the long experiment. This plant can be considered as a viable alternative biosorbent for use in metal removal treatment process for industrial effluents in wetlands.

Acknowledgment

We thank to the Brazilian Light Synchrotron Laboratory (LNLS) for partial financing of this study through the 6718 project.

References

[1] G. Blázquez, F. Hernáinz, M. Calero, L.F. Ruiz-Núñez, Removal of cadmium ions with olive stones: the effect of some parameters, Process Biochem. 40 (2005) 2649–2654.

[2] T. Bahadir, G. Bakan, L. Aitas, H. Buyukgungor, The investigation of lead removal by biosorption: an application at storage battery industry wastewaters, Enzyme Microb. Technol. 41 (2007) 98–102.

[3] O.M.M. Freitas, R.J.E. Martins, C.M. Delerue-Matos, R.A.R. Boaventura, Removal of Cd(II), Zn(II) and Pb(II) from aqueous solutions by brown marine macro algae: kinetic modelling, J. Hazard. Mater. 153 (2008) 493–501.

[4] F. Veglio, F. Beolchini, Removal of metals by biosorption: a review, Hydrometallurgy 44 (1997) 301–316.

[5] A.P. Terry, W. Stone, Biosorption of cadmium and copper contaminated water by *Scenedesmus abundans*, Chemosphere 47 (2002) 249–255.

[6] S.G. Kim, J.H. Jee, J.C. Kang, Cadmium accumulation and elimination in tissues of juvenile olive flounder, *Paralichthys olivaceus* after sub-chronic cadmium exposure, Environ. Pollut. 127 (2004) 117–123.

[7] P. Miretzky, A. Saralegui, A.F. Cirelli, Aquatic macrophytes potential for the simultaneous removal of heavy metals (Buenos Aires, Argentina), Chemosphere 57 (2004) 997–1005.

[8] G. Yan, T. Viraraghavan, Heavy-metal removal from aqueous solution by fungus *Mucor rouxii*, Water Res. 37 (2003) 4486–4496.

[9] M.A. Hashim, K.H. Chu, Biosorption of cadmium by brown, green, and red seaweeds, Chem. Eng. J. 97 (2004) 249–295.

[10] U.N. Rai, S. Sinha, R.D. Tripathi, P. Chandra, Wastewater treatability potential of some aquatic macrophytes: removal of heavy metals, Ecol. Eng. 5 (1995) 5–12.

[11] K.R. Reddy, Fate of nitrogen and phosphorus in a waste-water retention reservoir containing aquatic macrophytes, J. Environ. Qual. 12 (1983) 137–141.

[12] R.M. Gersberg, B.V. Elkins, S.R. Lyon, C.R. Goldman, Role of aquatic plants in wastewater treatment by artificial wetlands, Water Res. 20 (1986) 363–368.

[13] F.R. Espinoza-Quiñones, E.A. Silva, M.A. Rizzutto, S.M. Palácio, A.N. Módenes, N. Szymanski, N. Martin, A.D. Kroumov, Chromium ions phytoaccumulation by three floating aquatic macrophytes from a nutrient medium, World J. Microb. Technol. 24 (2008) 3063–3070.

[14] R.B. Clark, Characterization of phosphates in intact maize roots, J. Agric. Food Chem. 23 (1975) 458–460.

[15] Y. Yoneda, T. Horiuchi, Optical flats for use in X-ray spectrochemical microanalysis, Rev. Sci. Instrum. 42 (1971) 169–170.

[16] H. Aiginger, P. Wobrauschek, A method for quantitative X-ray fluorescence analysis in the nanogram region, Nucl. Instrum. Methods 114 (1974) 157–158.

[17] R.P. Pettersson, M. Olsson, A nitric acid–hydrogen peroxide digestion method for trace element analysis of milligram amounts of plankton and periphyton by total-reflection X-ray fluorescence spectrometry, J. Anal. At. Spectrom. 13 (1998) 609–613.

[18] M.J. Salvador, S. Moreira, D.A. Dias, O.L.A.D. Zucchi, Determination of trace elements in *Alternanthera brasiliana* and *Pfaffia glabrata* by SRTXRF: application in environmental pollution control, Instrum. Sci. Technol. 32 (2004) 321–333.

[19] F.R. Espinoza-Quiñones, C.E. Zacarkim, S.M. Palácio, C.L. Obregón, D.C. Zenatti, R.M. Galante, N. Rossi, F.L. Rossi, I.R.A. Pereira, R.A. Welter, Removal of heavy metal from polluted river water using aquatic macrophytes salvinia sp., Braz. J. Phys. 35 (2005) 744–746.

[20] C.A. Pérez, M. Radtke, H.J. Sánchez, H. Tolentino, R.T. Neuenshwander, W. Barg, M. Rubio, M.I.S. Bueno, I.M. Raimundo, J.J.R. Rohwedder, Synchrotron radiation X-ray fluorescence at the LNLS: beamline instrumentation and experiments, X-Ray Spectrom. 28 (1998) 320–326.

[21] J. Kennedy, R. Eberhart, Swam Intelligence, Morgan Kaufmann, 2001.

[22] D.E.G. Trigueros, A.N. Módenes, A.D. Kroumov, Modeling biodegradation kinetics on benzene and toluene and their mixture, Bioautomation 7 (2007) 9–22.

[23] P. Van Espen, K. Janssens, I. Swenters, AXIL X-Ray Analysis Software, Canberra Packard, Benelux, 1986.

[24] S.M. Simabuco, E. Matsumoto, Synchrotron radiation total reflection for rain water analysis, Spectrochim. Acta B 55 (2000) 1173–1179.

[25] D. Schmitt, A. Müller, Z. Csögör, H.F. Frimmel, C. Posten, The adsorption kinetics of metal ions onto different microalgae and siliceous earth, Water Res. 35 (2001) (2001) 779–785.

[26] U. Borgmann, W.P. Norwood, D.G. Dixon, Re-evaluation of metal bioaccumulation and chronic toxicity in *Hyalella azteca* using saturation curves and the biotic ligand model, Environ. Pollut. 131 (2004) 469–484.